Supplement of Atmos. Chem. Phys., 20, 7617–7644, 2020
https://doi.org/10.5194/acp-20-7617-2020-supplement

Atmospheric Chemistry and Physics
Open Access
EGU

Supplement of

Propagation of gravity waves and its effects on pseudomomentum flux in a sudden stratospheric warming event

In-Sun Song et al.

Correspondence to: In-Sun Song (isong@kopri.re.kr)

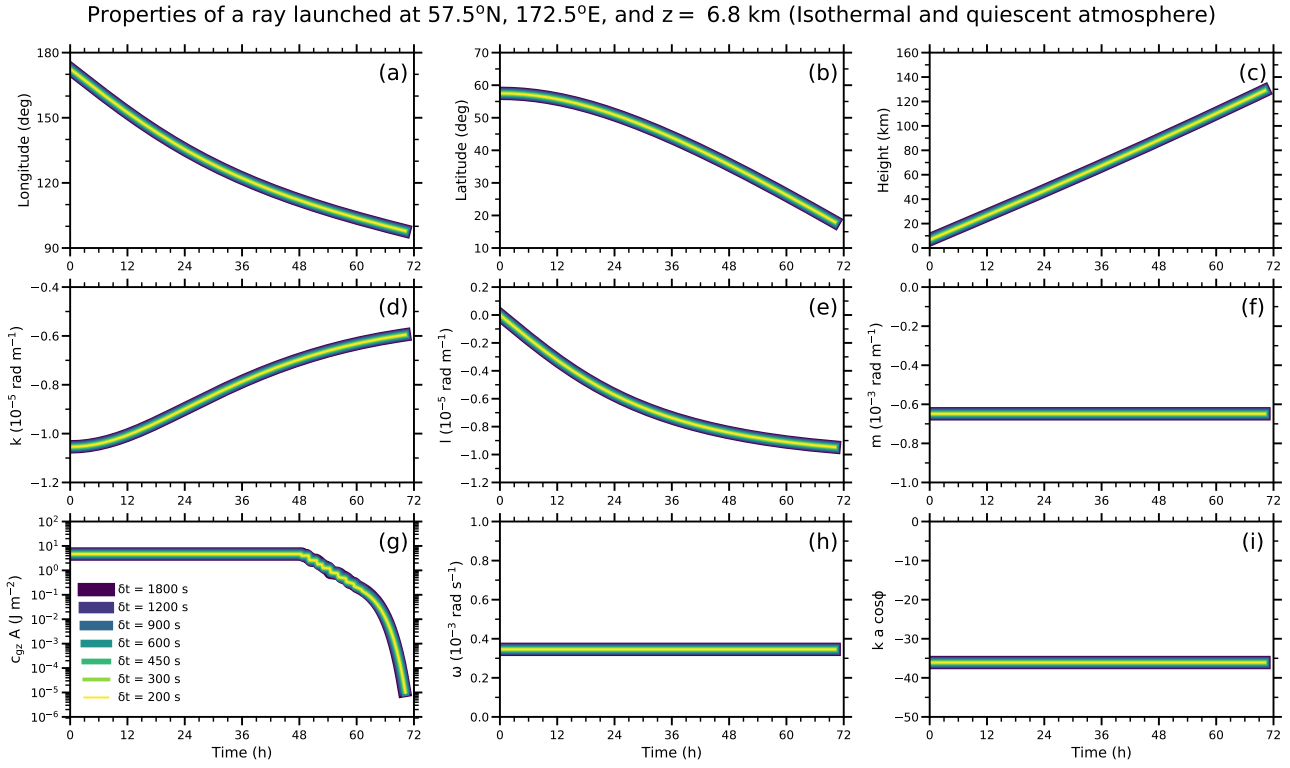

Figure S1. Time evolution of positions and properties of a ray launched at 57.5°N, 172.5°E, and $z = 6.8$ km in the isothermal and quiescent atmosphere for various timesteps (δt) from 200 s to 1800 s. For ray position, (a) longitude, (b) latitude, and (c) height are plotted. For ray's spectral properties and amplitudes, (d) zonal wavenumber (k), (e) meridional wavenumber (l), (f) vertical wavenumber (m), (g) wave action flux ($c_{gz}A$), (h) ground-based frequency (ω), and (i) zonal wavenumber multiplied by distance from the earth's rotation axis ($ka\cos\phi$) are plotted. This ideal test for single ray shows that positions and properties of the ray are almost independent of choice of timesteps (δt). At initial position and time, the ray has the horizontal wavelength of 596 km, the ground-based phase speed of 32.8 m s^{-1} in the westward direction, and the Reynolds stress ($\bar{\rho}\overline{u_h' w'}$) of 5.636×10^{-5} N m^{-2}, where $\bar{\rho}$ is the basic-state density, and u_h' and w' are the wave-induced horizontal and vertical wind perturbations, respectively. In the isothermal and quiescent atmosphere, the static stability and density scale height are constant, and horizontal wind components are zero. Therefore, there are no spatiotemporal gradients of the background flow. As a result, as the ray propagate upward (c), its horizontal positions follows a great circle path [(a)–(b)], vertical wavenumber and ground-based frequency are invariant [(f) and (h)], and horizontal wavenumber components are changed by the curvature terms alone [(d)–(e)]. Zonal wavenumber is changed in time due to the curvature term, but $ka\cos\phi$ is conserved (i). Therefore the vertical flux of the angular pseudomomentum ($kc_{gz}Aa\cos\phi$) is conserved unless the action flux ($c_{gz}A$) is diminished due to nonlinear saturation or molecular diffusion in the upper atmosphere [see $t < 48$ h in (g)]. The ray disappears around $t = 70$ h because $|\boldsymbol{k}_h c_{gz} A| < 10^{-10}$, which is one of ray termination conditions.

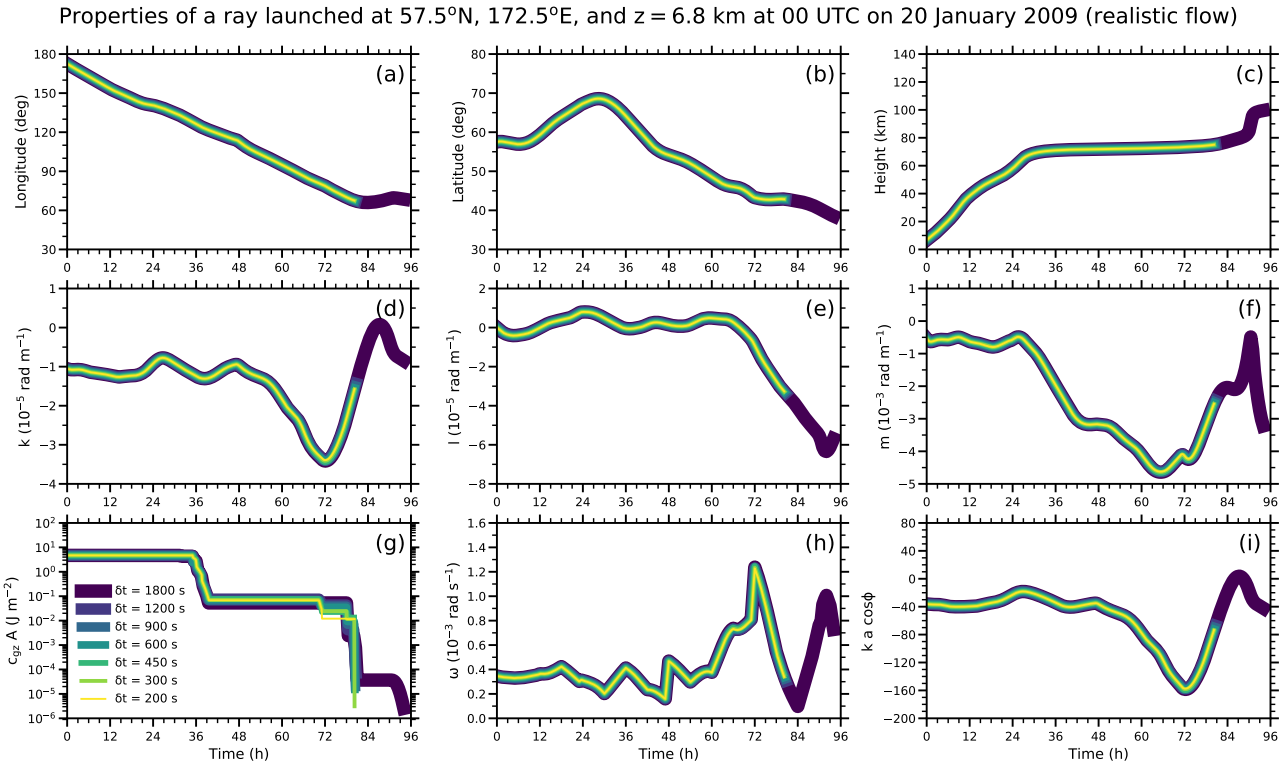

Figure S2. The same as Figure S1 except for realistic atmospheric flows specified at an hourly interval from 00 UTC on 20 January 2009. This single-ray test also shows that positions and properties of the ray do not depend significantly on timesteps (δt) for $\delta t \leq 900$ s. The vertical flux of the angular pseudomomentum ($kc_{gz}Aa\cos\phi$) is not conserved, even when the ray is not dissipated (see the invariance of $c_{gz}A$ for 0 h $\leq t \leq$ 33 h and 42 h $\leq t \leq$ 69 h). This is because there is non-negligible change in $ka\cos\phi$ due to the zonal variations of the large-scale flow and the meridional propagation of the ray.

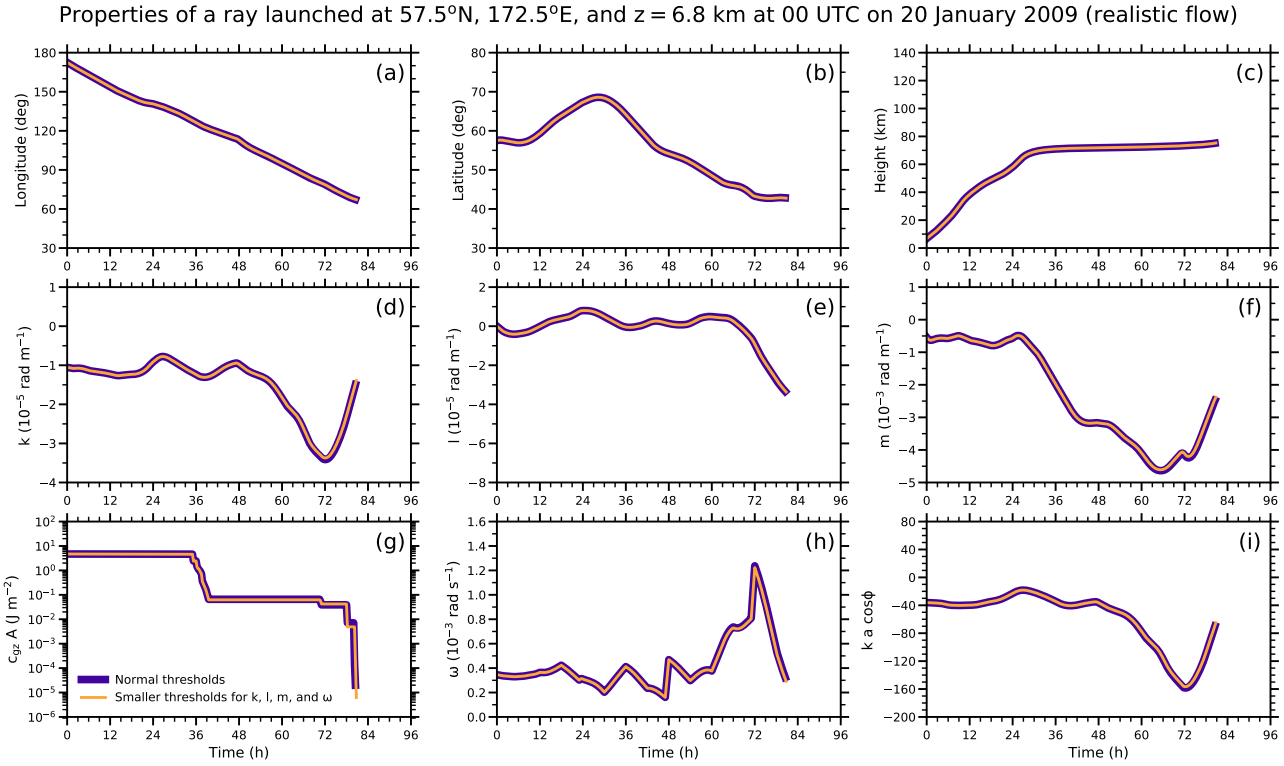

Figure S3. The same as Figure S2 except for using $\delta t = 900$ s and two different sets of thresholds in the LSODA. Normal thresholds indicates that default relative (absolute) thresholds of 10^{-3} and 10^{-6} (10^{-6} and 10^{-9}) are employed for position (λ, ϕ, and z) and spectral (k, l, m, and ω) variables, respectively (see Appendix A3 for details). For the other set of thresholds, the relative and absolute thresholds for spectral variables (k, l, m, and ω) are significantly reduced compared with the normal values and set equal to 10^{-15} and 10^{-18}, respectively.

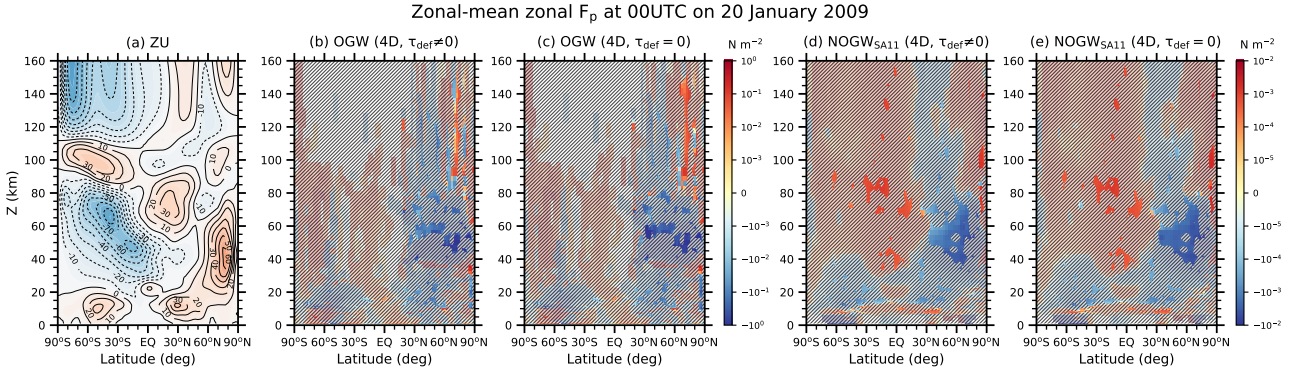

Figure S4. Latitude-height cross-sections of (a) zonal-mean zonal wind (ZU) and (b–e) zonal-mean zonal pseudomomentum fluxes (F_p) for OGWs and NOGW$_{SA11}$s in the 4D experiments with $\tau_{def} \neq 0$ and $\tau_{def} = 0$ at 00 UTC on 20 January 2009. OGW F_p is multiplied by the efficiency factor (0.125). Contour interval of zonal-mean zonal wind is 10 m s^{-1} and negative values are plotted in dashed lines. Hatched areas on the F_p indicate regions where the paired and two-tailed t-tests for 20 ensemble members of the two 4D experiments with $\tau_{def} \neq 0$ and $\tau_{def} = 0$ give p values larger than 0.05 (i.e., no statistical significance at the level of 0.05).

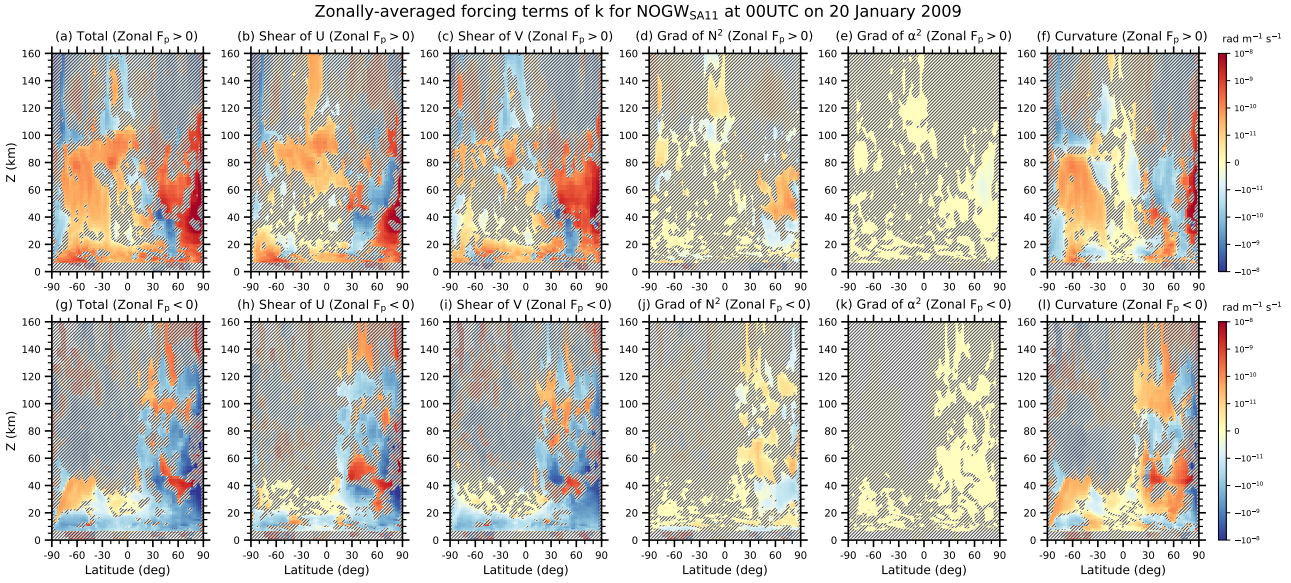

Figure S5. Latitude-height cross-sections of total and all the five forcing terms of zonal wavenumber for NOGW$_{SA11}$s with (top) eastward and (bottom) westward pseudomomentum fluxes in the 4D experiment at 00 UTC on 20 January 2009. The zonal shear terms of U and V are $-k/(a\cos\phi)\partial U/\partial\lambda$ and $-l/(a\cos\phi)\partial V/\partial\lambda$, respectively. Zonal gradient terms of N^2 and α^2 are $-k/(a\cos\phi)k_h^2/(2\hat{\omega}\sigma^2)\partial N^2/\partial\lambda$ and $k/(a\cos\phi)(\hat{\omega}^2 - f^2)/(2\hat{\omega}\sigma^2)\partial\alpha^2/\partial\lambda$, respectively. The curvature term is given by $lc_{g\lambda}\tan\phi/a$. Hatched areas indicate regions where the paired and two-tailed t-tests for 20 ensemble members of the 4D and 2D experiments give p values larger than 0.05 (i.e., no statistical significance at the level of 0.05).

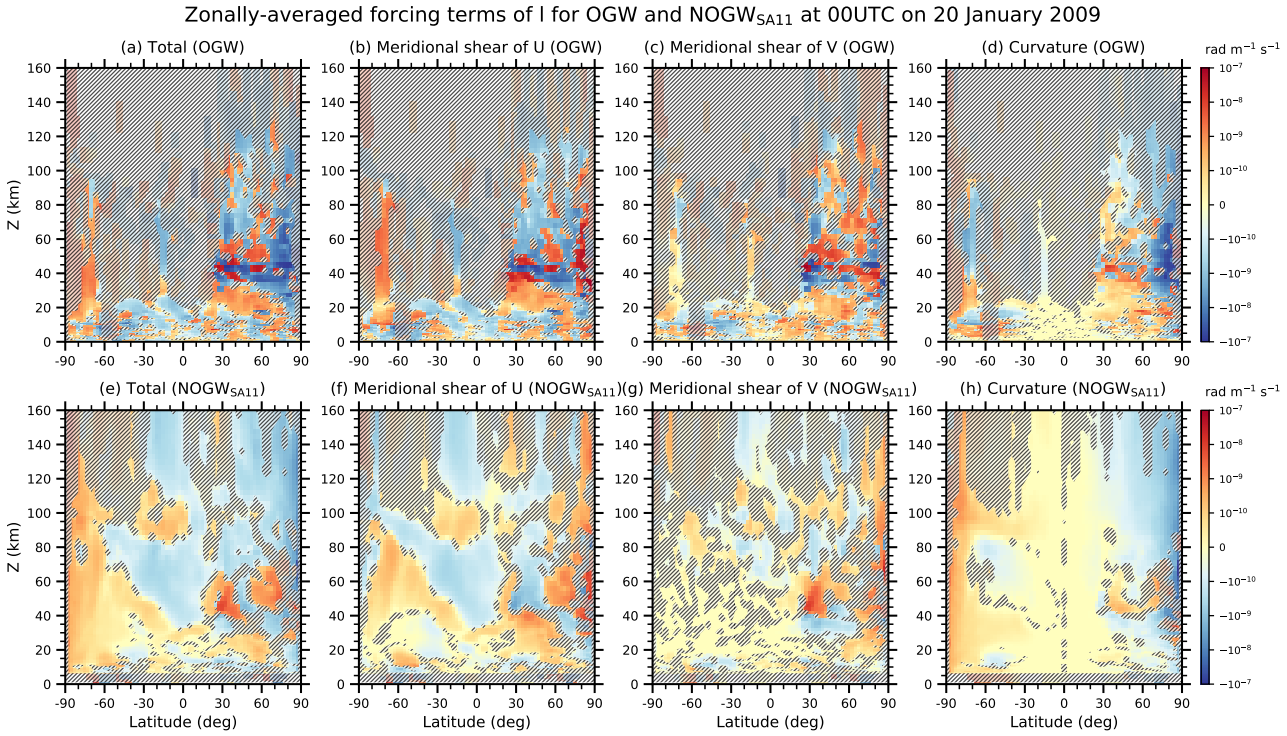

Figure S6. Latitude-height cross-sections of total and three major forcing terms [The meridional shear terms for the large-scale zonal and meridional winds (U and V) and the curvature term] of meridional wavenumber for (top) OGWs and (bottom) NOGW$_{\mathrm{SA11}}$s in the 4D experiment at 00 UTC on 20 January 2009. The meridional shear terms of U and V are $-(k/a)\partial U/\partial\phi$ and $-(l/a)\partial V/\partial\phi$, respectively. The curvature term is given by $-kc_{g\lambda}\tan\phi/a$. Hatched areas indicate regions where the paired and two-tailed t-tests for 20 ensemble members of the 4D and 2D experiments give p values larger than 0.05 (i.e., no statistical significance at the level of 0.05).

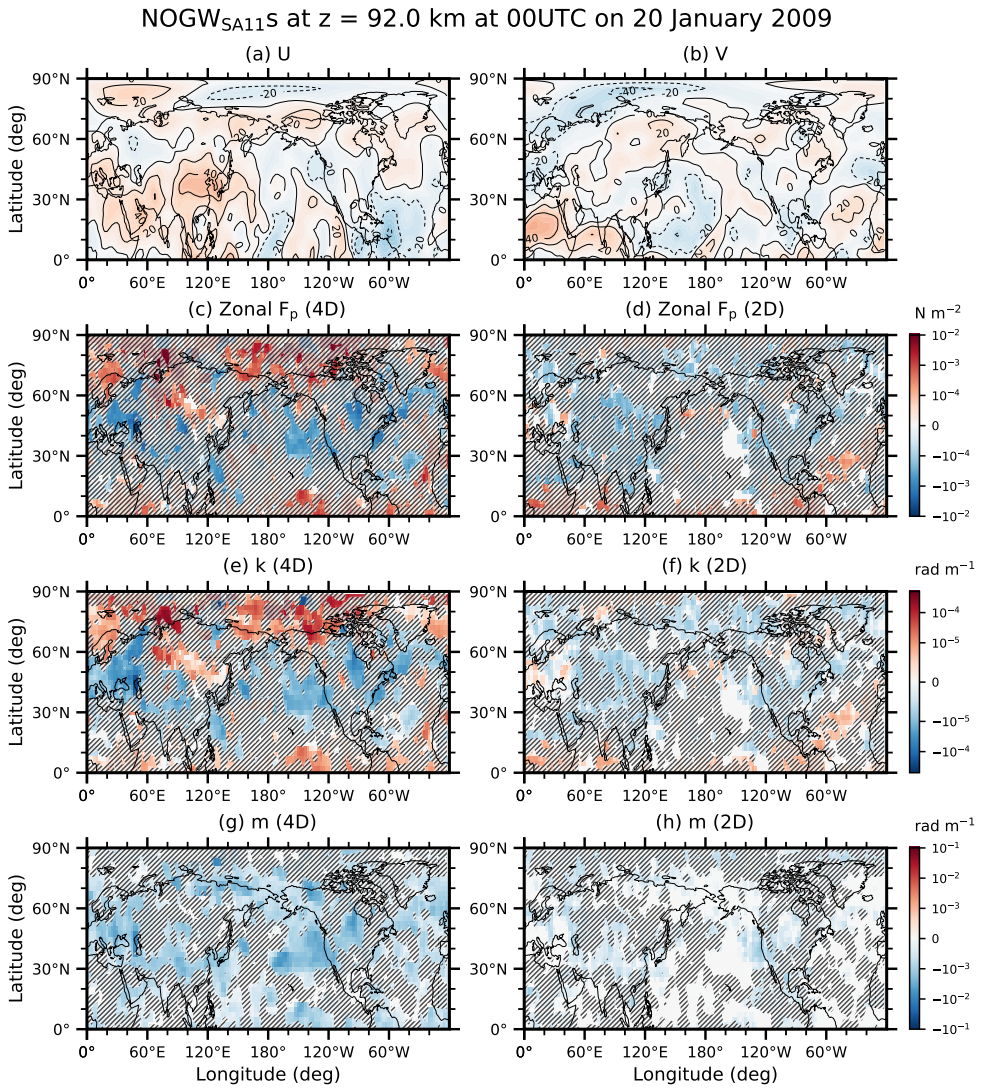

Figure S7. Longitude-latitude cross-sections of (a) zonal wind (U), (b) meridional wind (V), and ensemble means of (c–d) zonal pseudomomentum fluxes (F_p), (e–f) zonal wavenumbers and (g–h) vertical wavenumbers for NOGW$_{SA11}$s at $z = 92$ km in the 4D and 2D experiments at 00 UTC on 20 January, 2009. Contour interval for zonal and meridional winds is 10 m s^{-1} and negative values are plotted in dashed lines. Hatched areas indicate regions where the paired and two-tailed t-test for the 4D and 2D experiments gives p values larger than 0.05 (i.e., no statistical significance at the level of 0.05).

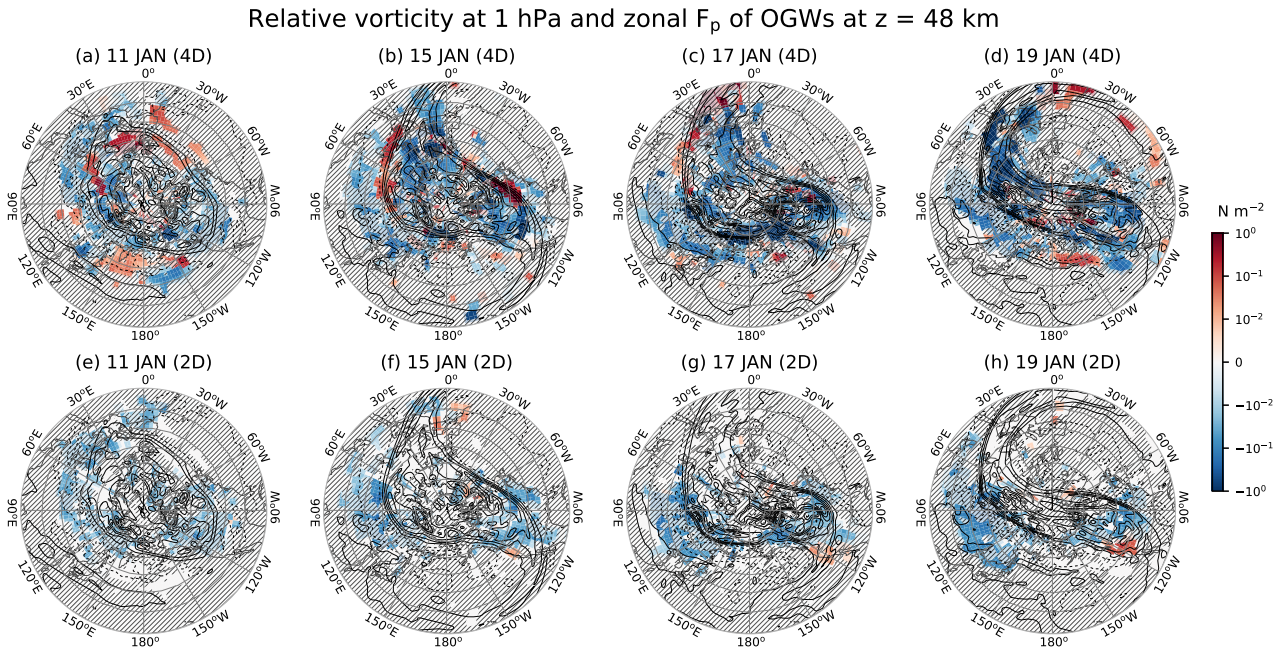

Figure S8. Relative vorticity at 1 hPa and zonal pseudomomentum fluxes (F_p) for OGWs at 00 UTC at $z = 48$ km on (a, e) 11 January, (b, f) 15 January, (c, g) 17 January, and (d, h) 19 January in 2009 for the (top) 4D and (bottom) 2D experiments. OGW F_p is multiplied by the efficiency factor (0.125). Contour interval for relative vorticity is 5×10^{-5} s^{-1} and negative values are plotted in dashed lines. Hatched areas over the zonal F_p indicate regions where the paired and two-tailed t-test for the 4D and 2D experiments gives p values larger than 0.05 (i.e., no statistical significance at the level of 0.05). Latitudinal grids are plotted every 10° from 20°N.

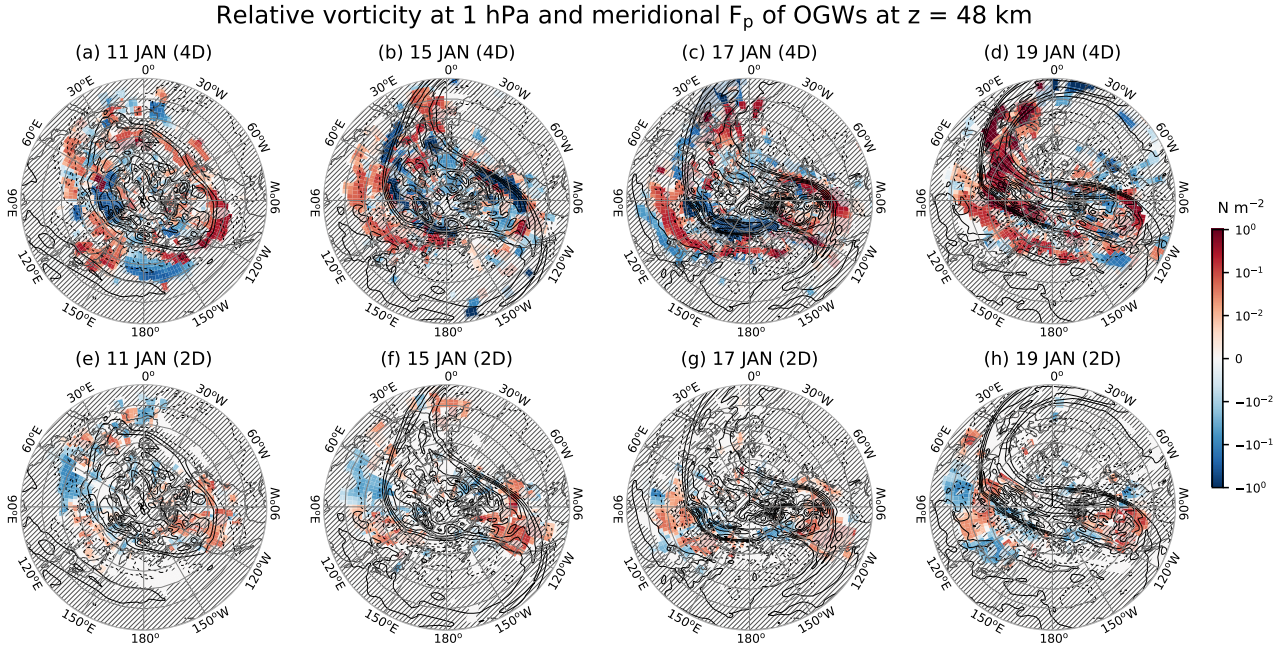

Figure S9. Same as Fig. S8 except for meridional pseudomomentum fluxes (F_p).

Table S1. Azimuthal angles, phase speeds, Reynolds stress, and horizontal wavelengths of NOGWs for SA11, WM96a, and WM96b

ID	Azimuth angle (°)	Phase speed (m s^{-1})	Reynolds stress (N m^{-2})	Horizontal wavelength (km)		
				SA11	WM96a	WM96b
1	0	6.8	1.29×10^{-3}	385	396	398
2	45	6.8	1.54×10^{-3}	410	439	472
3	90	10.2	1.41×10^{-3}	504	782	942
4	135	6.8	1.54×10^{-3}	570	439	472
5	180	6.8	1.82×10^{-3}	596	485	558
6	225	6.8	1.54×10^{-3}	570	439	472
7	270	10.2	1.41×10^{-3}	504	782	942
8	315	6.8	1.54×10^{-3}	410	439	472
9	0	32.8	4.00×10^{-5}	385	604	283
10	45	20.4	4.72×10^{-5}	410	309	128
11	135	20.4	4.72×10^{-5}	570	309	128
12	180	32.8	5.63×10^{-5}	596	741	397
13	225	20.4	4.72×10^{-5}	570	309	128
14	315	20.4	4.72×10^{-5}	410	309	128